

From Macro to Micro Plastics; Influence of Photo-oxidative Degradation

J. Papac Zjačić,^{a*} M. Vujasinović,^a M. Kovačić,^a A. Lončarić Božić,^a H. Kušić,^{a,b} Z. Katančić,^a and Z. Hrnjak Murgić^a

^a Department of Polymer Engineering and Organic Chemical Technology, Faculty of Chemical Engineering and Technology, University of Zagreb, Trg Marka Marulića 19, 10 000 Zagreb, Croatia

^b University North, Trg dr. Žarka Dolinara 1, 48 000 Koprivnica, Croatia

This work is licensed under a Creative Commons Attribution 4.0 International License



Abstract

The impact of plastic waste on the environment, human health, and ecosystems is one of the most important issues today. Once released into the environment, plastic waste is exposed to various stress factors that can lead to a reduction in its structural integrity and consequently to its fragmentation into smaller pieces. In this work, the effects of simulated UV aging on the surface properties and fragmentation of high-density polyethylene (HDPE) films were studied. HDPE films were prepared from pristine polymer granules, and aged for 14, 28, and 42 days under artificial UV irradiation. The samples were characterised before and after each irradiation period to inspect structural and surface changes. FTIR spectra revealed the appearance of carbonyl (C=O) and carbon-oxygen (C–O, O–C=O, C–O–O–) groups due to photodegradation of HDPE. The change in surface polarity with UV irradiation time was determined by measuring the water contact angle, while the surface morphology was analysed using a SEM microscope. The results revealed a significant increase in carbonyl index, increased hydrophilicity, and increased brittleness resulting from a high degree of photodegradation after 28 and 42 days of UV irradiation. The different particle size distribution yielded upon grinding indicated that aged HDPE films are more prone to fragmentation into micro-sized particles.

Keywords

Plastic waste, HDPE films, photodegradation, hydrophilicity – hydrophobicity, fragmentation

1 Introduction

The large-scale production and increasing consumption of plastic materials raises concern for human health and the sustainability of ecosystems. Thus, the global plastics production was estimated to have reached 367 million metric tons in 2020, and continuous growth in production and market value is expected. The global plastics market was valued at 593 billion U.S. dollars in 2021, and the market is projected to grow in the coming years to reach a value of more than 810 billion U.S. dollars by 2030.^{1,2} Plastic production is set to continue growing due to rising populations, increased buying power, and further demands for plastic goods. The incredible versatility of this group of materials accounts for its continued growth, because they offer many advantages; they are extremely lightweight, have good physical, mechanical, and chemical properties, can be easily shaped into complex forms and are affordably priced.^{3,4} Therefore, plastic materials are especially widely used as packaging materials, and packaging waste accounts for 36 % of solid waste in EU, with plastics being the most widely used material in European food retail, covering 37 % of food sold. Between 75–112 billion EUR worth of plastic packaging material is lost from the economy each year, which is equivalent to the GDPs of both Slovakia and Hungary combined.⁵ Plastic is indeed a key material in packaging, due to its lightweight, durability, and unparalleled flexibility in shapes, colours, properties, and functions. Its various barrier properties allow for food preservation

by extending shelf life. All these benefits come at a price low enough for the entire packaging industry, especially the food and cosmetics industries, to build economically sustainable value chains. Recent research⁶ indicates that significant reductions can be achieved by focusing on six polymers used for multilayer/multimaterial flexibles, business-to-business packaging, films, bottles, carrier bags, and foodservice disposables, which are projected to account for 86 % of the total reduction achievable by 2040, Table 1.

Table 1 – Six polymers most commonly used
Tablica 1 – Šest polimera koji su najčešće u upotrebi

POLYMER	ABBREVIATION	SYMBOL
Poly(ethylene terephthalate)	PET	
Polyethylene high density	HDPE	
Poly(vinyl chloride)	PVC	
Polyethylene low density	LDPE	
Polypropylene	PP	
Polystyrene	PS	

* Corresponding author: Josipa Papac Zjačić, mag. ing. oecoiing.
Email: jpapac@fkit.unizg.hr

The major issue with plastic products and waste is their heterogeneity, which significantly reduces their recyclability due to their different properties. Thus, polyethylene terephthalate (PET) polymer has a melting point at 250 °C, high-density polyethylene (HDPE) at 130 °C, low-density polyethylene (LDPE) at 120 °C, PP at 160 °C, poly(vinyl chloride) (PVC) between 100 and 260 °C, and polystyrene (PS) at approximately 240 °C.⁷ Due to their different melting temperatures, it is not possible to mechanically recycle these polymers together. For example, the mixture of PET and HDPE cannot be recycled by extrusion, because melting of PET requires high temperatures, which cause degradation of HDPE. In addition, heterogeneity implies a different chemical composition that significantly affects the recycling process, whether it is chemical or mechanical recycling. Thus, the energy recovery of mixed plastic waste by incineration is one of the profitable forms of recycling. This is the method used by highly developed EU countries in managing mixed plastic waste.⁸ The problem occurs in underdeveloped countries that lack a system of separate waste collection, and are unable to afford the construction of expensive infrastructure. Most plastic waste ends up in the environment, posing a threat to human health and living organisms. These issues indicate unsustainable practice, as plastic persists in the environment for long periods since it is non-biodegradable. Additionally, a significant amount of waste from the environment reaches the seas and oceans through rainwater and rivers.⁹ Therefore, the solutions and answers to the problem of excessive plastic usage need to be given at several different levels. These are: a) separate waste collection, b) development of returnable plastic packaging, c) packaging refill, d) reduction of polymer types, and e) replacement of plastics with biodegradable materials, all of which can be accomplished through regulations and adoption of new social behaviours. Solutions that solely involve replacing plastics with other materials are not satisfactory since the problem of excessive waste disposal remains. Thus, the most viable solution from environmental, economic, and social perspectives would be an immediate reduction in plastic production – through elimination, substitution, and expansion of consumer reuse options. This would enable the largest reduction in plastic pollution, often yield net environmental savings, and offer the highest potential for mitigating greenhouse gas (GHG) emissions compared to existing alternative system interventions (such as mechanical recycling or plastic to plastic chemical conversion).^{6,10}

Furthermore, there is the problem of plastic accumulation in the environment, because the vast amount of plastic covers large surface areas, thus preventing the growth of living organisms and plants, and often end up in water systems. In addition, the problem of the long duration of plastic in the environment causes its fragmentation into smaller particles forming microplastics (MPs). Weathering and particularly exposure to UV irradiation from the sun cause photodegradation of plastics resulting in deterioration of the material properties, especially mechanical properties, like high brittleness, initiating formation of MPs. Such small particles, smaller than 5 mm, can be ingested by various organisms living in water, ultimately endangering human health as we are at the end of the food chain.^{9,11} It should be pointed out that plastic materials are not usually toxic,

but some may contain additives such as stabilisers, flame retardants, pigments, and fillers or residual monomers. All these non-polymeric components are usually of low molecular weight and may, therefore, migrate from the plastic product to air, water or other contact media (e.g., food).¹² In the environment, various toxic substances such as organic and inorganic contaminants, can adsorb onto microplastic surfaces through different interactions, as shown in Fig. 1. The adsorption capacity significantly increases when plastic is transformed into MPs due to the high ratiion size and particle surface. Because of the potential threat of toxic additives and adsorbed substances onto MPs, it is necessary to examine their deposition in humans, living organisms, and the environment.^{13,14}

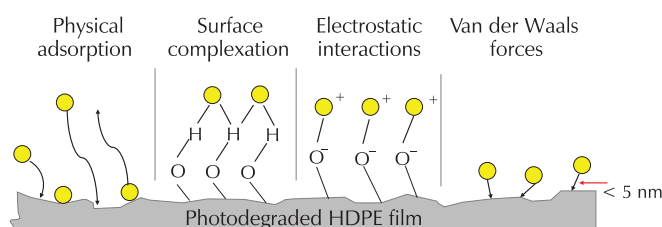


Fig. 1 – Adsorption and interaction between plastic surface and contaminants (yellow circles) in the environment

Slika 1 – Adsorpcija i interakcije između površine plastike i onečišćivala (žuti krugovi) u okolišu

PE is one of the most inert polyolefins; however, it does degrade very slowly in the natural environment. Generally, PE successfully resists photo-oxidative degradation due to the lack of UV-VIS chromophores, because its backbone chains are constructed exclusively from C–C single bonds. Usually, impurities or structural defects formed in PE during its manufacturing, or during later weathering¹⁵, act as chromophores¹⁶, but also a small number of unsaturated (C=C) double bonds in the main chain or at the chain ends (vinyl in HDPE and vinylidenes groups in LDPE). Also, low-density polyethylene (LDPE) in comparison to high-density polyethylene (HDPE) possesses a higher frequency of reactivity due to branch points in the low-density polymer.¹⁷ All these sites are readily oxidised by O₂ after light is absorbed in photo-oxidative degradation to initiate chain reactions.¹⁸ The resulting degradation products formed in both photo-oxidative and thermal processes are similar (Fig. 2).

Photo-oxidative degradation begins with absorbed light and abstraction of hydrogen atom from the PE chain, forming a reactive carbon alkyl radical. The alkyl radical captures O₂ and forms a peroxy radical, which abstracts another hydrogen atom from the new polymer chain and proceeds through the formation of a hydroperoxide and a new alkyl radical. The hydroperoxide O–O bond scission leads to alkoxy and hydroxyl radicals, each of which can abstract another hydrogen atom and generate a new alkyl radical. Finally, termination of the radical chain mechanism occurs through bimolecular radical recombination.¹⁹ The stable final products are ketones and water molecules, while hydroperoxides, hydroxyl radicals, and peroxy rad-

icals continue with further reactions, together with alkyl and alkoxy radicals.

The aim of this study was to investigate UV-induced changes in HDPE properties influencing its fragmentation into MPs. For that purpose, HDPE films were exposed to UV irradiation for 14, 28, and 42 days, and chemical and morphological changes were investigated. Different particle size distributions obtained upon grinding were correlated with the rate of photo-oxidative degradation of HDPE films.

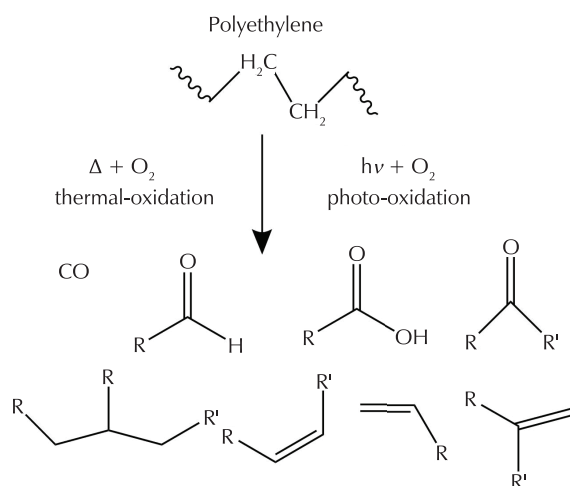


Fig. 2 – Products formed in photo- and thermal-oxidative degradation of PE (R, R', R'' are polymer chains of various lengths)

Slika 2 – Produkti nastali tijekom foto i termooksidativne razgradnje PE (R, R', R'' su polimerni lanci različitih duljina)

2 Experimental

2.1 Material

Granules of HDPE (EGDA-6888 Natural) density 0.952 g cm^{-3} , melt flow rate 10 g min^{-1} , were used to prepare films of 0.5 mm thickness. Films were prepared by pressing in a mould of dimensions $60 \times 10 \times 0.5 \text{ mm}$. The process was carried out in two steps. Firstly, the granules were heated to $180 \text{ }^\circ\text{C}$ for 3 min to melt, and then pressed at 15 bar for the next 3 min by hydraulic press Fontijne. The samples were then transferred to cold hydraulic press Dake to cool down under pressure of 5 bar for another 10 min.

2.2 Photo-oxidation

HDPE films were subjected to artificial accelerated ageing conducted in a Heraeus Instruments Suntest, CPS chamber with xenon lamps, air-cooled. The test chamber was equipped with cut-off filter, which removed UV-C irradiation below 290 nm, simulating solar irradiation outdoors, while the chamber temperature was controlled at $45 \pm 1 \text{ }^\circ\text{C}$ with a relative humidity below ambient due to

the elevated temperature. Samples were fastened in the chamber and exposed to UV irradiation for 14, 28, and 42 days.

2.3 Grinding into microplastics

After UV irradiation, the samples were ground in a drum cryogenic mill, Retsch CryoMill. The grinding was performed in three cycles, and each cycle consisted of three steps: precooling (frequency = 5 s^{-1} ; $t = 1 \text{ min}$), grinding (frequency = 25 s^{-1} ; $t = 1 \text{ min}$), and intercooling (frequency = 5 s^{-1} ; $t = 30 \text{ s}$). The particle size distributions of the obtained MPs were determined by sieving using five sieves with different mesh sizes, on a Sieve Shaker AS 200 control – RETSCH. The size ranges of microplastic fractions were: $> 500 \text{ } \mu\text{m}$, $400\text{--}500 \text{ } \mu\text{m}$, $300\text{--}400 \text{ } \mu\text{m}$, $200\text{--}300 \text{ } \mu\text{m}$, $100\text{--}200 \text{ } \mu\text{m}$, and $< 100 \text{ } \mu\text{m}$, and mass of each fraction was determined gravimetrically.

2.4 Characterisation

FTIR spectroscopy. FTIR spectra of HDPE samples before and after UV irradiation were recorded using a Perkin Elmer Spectrum One spectrometer in ATR mode equipped with ZnSe crystal. Measuring range was from 4000 to 650 cm^{-1} with a 4 cm^{-1} resolution. FTIR spectra were measured in three different areas, and average spectra are presented to avoid possible uneven surface degradation.

As an indicator of degradation and chemical changes with UV ageing, the indices of carbon-oxygen bonds (C–O) and carbonyl group bonds (C=O) were monitored, and carbonyl index (C.I.) was calculated. The C.I. was calculated from the ratio between the integrated band absorbance of the carbonyl (C=O) peak from 1850 to 1650 cm^{-1} and that of the methylene (CH₂) scissoring peak from 1500 to 1425 cm^{-1} , as expressed in the following equation:²⁰

$$\text{C.I. (C = O)} = \frac{\text{area under band } A_{1850-1650 \text{ cm}^{-1}}}{\text{area under band } A_{1500-1425 \text{ cm}^{-1}}} \quad (1)$$

For the carbon-oxygen bonds, peaks from 1300 to 1140 cm^{-1} were taken and expressed in the following equation:²¹

$$\text{C.I. (C - O)} = \frac{\text{area under band } A_{1300-1140 \text{ cm}^{-1}}}{\text{area under band } A_{1500-1425 \text{ cm}^{-1}}} \quad (2)$$

The area under the band was calculated using the peak analysis tool of the Perkin Elmer Instrument software options.

Differential scanning calorimetry (DSC). Mettler Toledo DSC 823eT was used to characterise HDPE films. The heating/cooling rate was $10 \text{ }^\circ\text{C min}^{-1}$ in the range from 20 to $200 \text{ }^\circ\text{C}$. The crystallisation degree (X_c) was determined as a ratio of the melting enthalpy (ΔH_m) and melting enthalpy (ΔH_m^0) for 100 % crystalline HDPE obtained from literature.²²

$$X_c = \frac{\Delta H_m}{\Delta H_m^0} \quad (3)$$

Contact angle measurement. Surface properties of the studied samples were monitored using Data Physics OCA20 goniometer to determine the contact angle (θ). The measurements were performed at room temperature for five replicates, test liquid was water, pH 7.0 from Milli-Q, and a sessile drop of 2 μl volume was used.

Scanning Electron Microscopy (SEM). The surface morphology and microstructure of studied samples were examined by SEM, Tescan Vega III, operated with a 10 kV voltage. In order to achieve surface conductivity, the samples were coated with Gold/Palladium using SC7620-Mini Sputter Coater/Glow Discharge System.

3 Results and discussion

3.1 FTIR analysis

The photo-oxidative degradation of the studied HDPE films was examined with FTIR to monitor changes in the macromolecular structure. Fig. 3 presents FTIR spectra of HDPE films before and after 14, 28, and 42 days of exposure to UV irradiation. Photo-oxidative degradation of polyethylene resulted in the appearance of peaks at 1715 cm^{-1} and $1230\text{--}1180\text{ cm}^{-1}$, which were attributed to the newly formed chemical structures, namely, ketones ($\text{C}=\text{O}$) (expanded view in Fig. 4a) and carbon-oxygen groups ($\text{C}-\text{O}$, $\text{O}-\text{C}=\text{O}$, $\text{C}-\text{O}-\text{O}-$) (expanded view in Fig. 4b).

As may be seen in Figs. 4a and 4b, the increase in intensity of $\text{C}=\text{O}$ bands centred around 1715 cm^{-1} , and $\text{C}-\text{O}$ bands around 1180 cm^{-1} , between 0 and 14 days of UV irradiation, is less pronounced than in the subsequent time

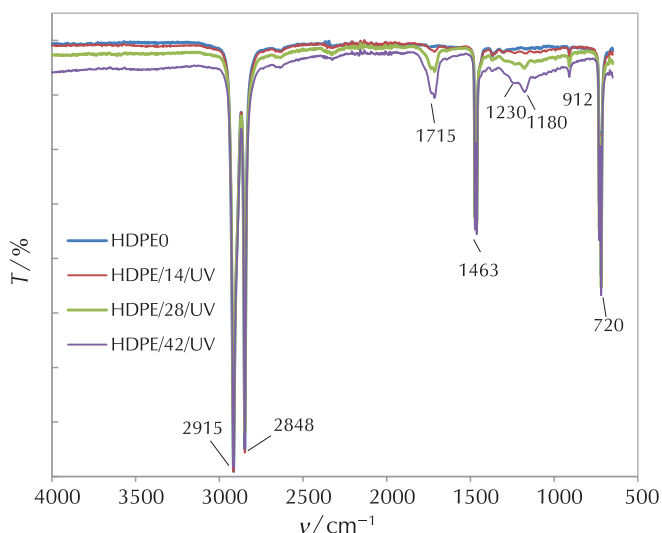


Fig. 3 – FTIR spectra of HDPE films UV-irradiated for 0, 14, 28, and 42 days

Slika 3 – FTIR spektri HDPE filmova UV ozračenih tijekom 0, 14, 28 i 42 dana

periods. This can be attributed to the initial stability of polyethylene. Once the first $\text{C}=\text{O}$ bonds appear, they act as chromophores, which more readily absorb UV irradiation and accelerate the process. The peak at 1715 cm^{-1} is attributed to the ketone group, while the shoulder visible at 1733 cm^{-1} belongs to aliphatic ester groups.²²

Table 2 lists the indices of the carbonyl index calculated for $\text{C}=\text{O}$ and $\text{C}-\text{O}$ groups using the value of the reference peaks in the range from 1500 to 1425 cm^{-1} . In addition, the indices were determined for the upper side of the film ($\text{HDPE}/x/\text{U}$) exposed to UV irradiation, as well as for the bottom side ($\text{HDPE}/x/\text{B}$) of the samples to determine if UV

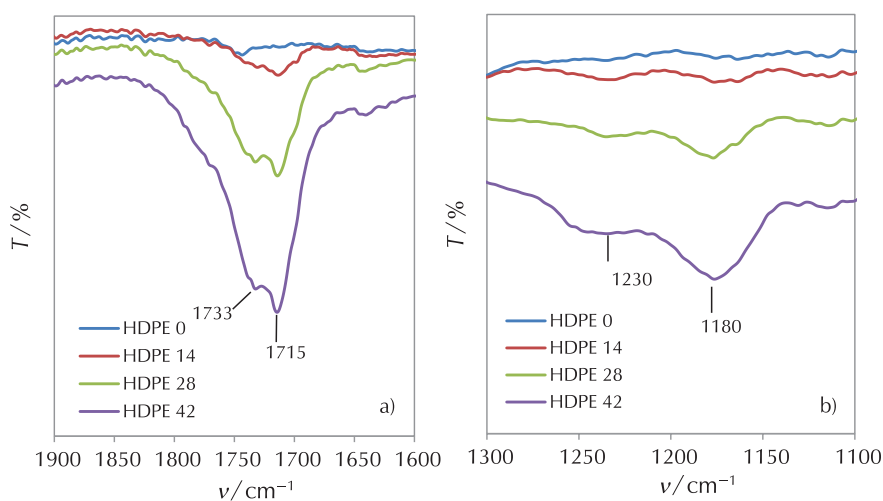


Fig. 4 – FTIR spectra of HDPE films UV-irradiated for 0, 14, 28, and 42 days; a) peaks in the region of carbonyl bond and b) peaks in the region of carbon-oxygen bonds

Slika 4 – FTIR spektri HDPE filmova UV ozračenih tijekom 0, 14, 28 i 42 dana; a) pikovi u području karbonilne skupine i b) pikovi u području skupine ugljik-kisik

Table 2 – Indices for carbonyl (C=O, 1715 cm⁻¹) and carbon-oxygen group (C–O, 1180, 1230 cm⁻¹) of pristine and UV-irradiated HDPE samples

Tablica 2 – Indikatori karbonilne (C=O, 1715 cm⁻¹) i skupine ugljik-kisik (C–O, 1180, 1230 cm⁻¹) početnog i ostarenih HDPE uzoraka

Sample	C=O 1850–1650	C–O 1300–1140	Sample	C=O 1850–1650	C–O 1300–1140
HDPE/0	$7.8 \cdot 10^{-4}$	0.007	HDPE/0	$7.8 \cdot 10^{-4}$	0.007
HDPE/14/U	0.088	0.036	HDPE/14/B	0.094	0.058
HDPE/28/U	0.195	0.044	HDPE/28/B	0.517	0.209
HDPE/42/U	0.276	0.352	HDPE/42/B	1.014	0.415

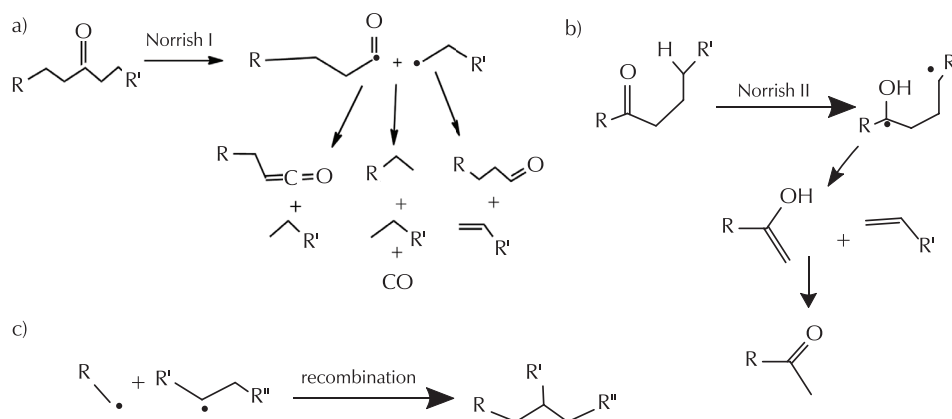


Fig. 5 – Photo-oxidative degradation of PE containing carbonyl impurities, via: a) a Norrish type mechanism or b) a Norrish II type mechanism, c) radical recombination to form cross-linked chains. R, R', R'' are polymer chains of varying lengths²⁷

Slika 5 – Fotooksidativna degradacija PE koji sadrži karbonilna onečišćenja: a) mehanizmom Norrish tip I ili b) mehanizmom Norrish tip II, c) radikalskom rekombinacijom kojom se formiraju umreženi lanci. R, R', R'' polimerni su lanci različitih duljina²⁷

irradiation penetrated the entire thickness of the film. The index calculated for the C=O groups region showed a significant increase on the upper side, with a regular trend as irradiation time increased. A similar, but slightly different trend was observed for the C–O groups. In this case, the index did not change significantly in the first 28 days, but rose sharply afterward, and the final value was higher than that for C=O groups. Such behaviour points to prevailing Norrish-type I reactions (Fig. 5a) in the first 28 days, in which photochemically induced homolytic scission leads to free radical intermediates, as well as Norrish-type II reactions after 28 days, in which ketones and vinylidene are formed by intramolecular γ -H abstraction (Fig. 5b).^{23,24} The rate of degradation is highly dependent on the amorphous fraction of the polymer. Thus, degradation is far slower in crystalline part of HDPE, because its lower chain mobility promotes recombination of radicals at the expense of radical propagation reactions.²⁵

Interestingly, the indices determined for the bottom surface of the samples (HDPE/x/B) showed an even higher increase with exposure time, *i.e.*, index for C=O groups after 42 days was four times higher than that for the upper side; 1.014 vs. 0.276. A similar trend was observed for the C–O group index. This can possibly be explained by simultaneous effects of photo-oxidative and thermo-oxidative deg-

radation arising from the mounting of the samples in UV chamber. The interior of the chamber was ventilated by strong fans to prevent overheating of the samples, and the temperature was maintained constantly at around 45 °C. To keep light polymer films in place, strong NdFeB magnets were used to fasten them to the metal surface below. Absorption of the irradiation by metal probably caused strong heating of the surface, which transferred excess heat to the bottom side of the polymer films and caused thermo-oxidative degradation. This, in combination with the penetration of UV light from the upper side, resulted in higher degradation from the bottom side.

3.2 DSC analysis

In order to obtain better insight into the UV irradiation-induced structural changes of HDPE, the DSC method was used, the results of which are presented in Table 3 and Fig. 6. Although for melting behaviour, the second heating cycle is usually used to erase thermal history of the sample, in this case, only the first heating run was used to observe direct influence of UV ageing. From the crystallisation temperature (T_c), it can be observed that the values decreased slightly from 110.7 to 105.6 °C with UV ageing, while

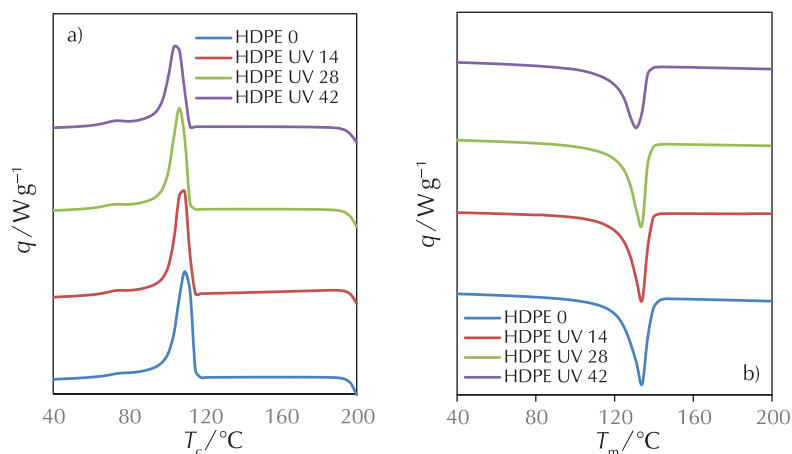


Fig. 6 – DSC thermograms of HDPE samples, pristine and UV-irradiated for 14, 28, and 42 days: a) crystallisation temperature (T_c) and b) melting temperature (T_m)

Slika 6 – DSC termogrami početnog HDPE uzorka i uzoraka ostarenih 14, 28 i 42 dana: a) temperatura kristalizacije (T_c) i b) temperatura taljenja (T_m)

the melting temperature (T_m) increased slightly (132.6 to 135.6 °C). The crystallisation enthalpy (ΔH_c) decreased with UV ageing (148.9 to 105.8 J g⁻¹), corresponding to a 30 % lower value, while the melting enthalpy (ΔH_m) increased around 10 %. All changes in thermal properties indicated a structural change with prolonged UV ageing, which was also well observed from the crystallisation degree (X_c) as an increase in crystallisation. This would suggest a decrease in molecular weight of the HDPE, which would allow easier stacking of shorter polymer chains into crystallites.²⁸

Table 3 – Crystallisation temperature (T_c), b) melting temperature (T_m), crystallisation enthalpy (ΔH_c), melting enthalpy (ΔH_m), and crystallisation degree (X_c) of pristine and UV irradiated HDPE samples

Tablica 3 – Temperatura kristalizacije (T_c), b) temperatura taljenja (T_m), entalpija kristalizacije (ΔH_c), entalpija taljenja (ΔH_m) i stupanj kristalizacije (X_c) početnog i ostarenih HDPE uzoraka

	HDPE 0	HDPE UV 14	HDPE UV 28	HDPE UV 42
$T_c/^\circ\text{C}$	110.7	109.2	107.5	105.6
$T_m/^\circ\text{C}$	132.6	133.3	134.3	135.6
$\Delta H_c/\text{J g}^{-1}$	148.9	137.3	125.8	105.8
$\Delta H_m/\text{J g}^{-1}$	156.2	158.2	169.5	170.2
$X_c/\%$	53.3	54.0	57.8	58.1

3.3 Surface characterisation

Possible surface changes caused by photo-oxidation were examined by water contact angle measurements and SEM images. Fig. 7 depicts surface-wetting characterisation of HDPE films using the water-contact angle measurement.

It can be seen that the tendency of water to spread and adhere to the surface of the HDPE/0 film is lower compared to aged HDPE films. This observation clearly indicates a positive correlation between hydrophilicity and photo-oxidative degradation of polymer films. Namely, the water-contact angle values changed from $97 \pm 1^\circ$ for the pristine HDPE/0 to $82 \pm 1^\circ$ for HDPE/42, which corresponds to a 15 % decrease during the observed period of accelerated aging. Such behaviour can be attributed to the formation of oxygen-containing functional groups, as revealed by previously discussed FTIR spectra.

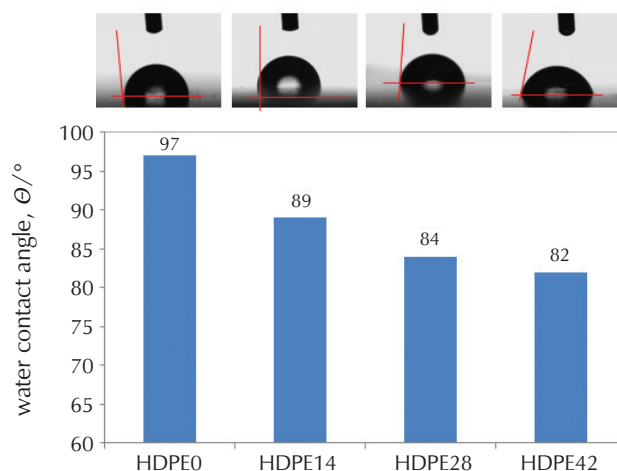


Fig. 7 – Water contact angles of HDPE films UV-irradiated for 0, 14, 28, and 42 days

Slika 7 – Kontaktni kut vode na HDPE filmovima nakon UV-ozračivanja 0, 14, 28 i 42 dana

The FTIR surface analysis revealed significant physico-chemical changes in the HDPE films due to aging. The

spectra revealed new peaks for carbonyl and carbon-oxygen groups observed after photodegradation, which increased the surface polarity of the films.

HDPE films were inspected for changes in surface morphology and roughness by SEM microscope before and after UV irradiation, and the microscopic images are shown in Fig. 8. On the surface, some scratches and scars can be seen for all samples, especially at higher magnifications (10,000 \times). These scratches can be attributed to imperfections of the steel moulds used in the preparation of the films, which left imprints on the surface. The microscopic images of the surface morphology show no significant changes with irradiation time, as could be expected from the degradation shown by the FTIR analysis. Only traces of surface degradation are visible as small cracks for the sample HDPE/42 at 10,000 \times magnification, marked in yellow. It is also evident that the photodegradation caused cracks on the surface and increased the brittleness of the polymer, as was later observed during grinding in a cryogenic mill.

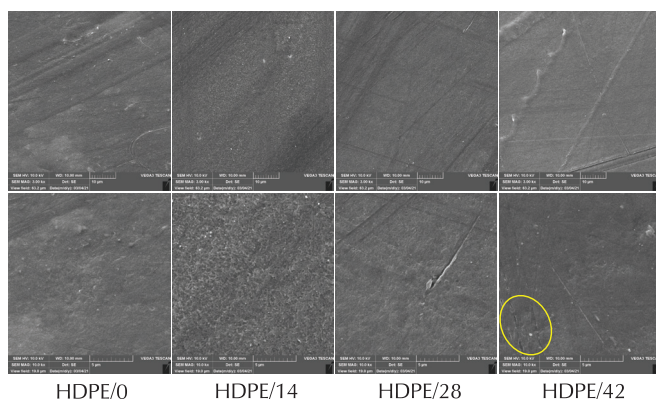


Fig. 8 – SEM micrographs of HDPE films UV-irradiated for 0, 14, 28, and 42 days; top row magnification 3,000 \times , bottom row magnification 10,000 \times

Slika 8 – SEM mikrofografije HDPE filmova UV-ozračenih tijekom 0, 14, 28 i 42 dana; gornji red uvećanje 3000 \times , donji red uvećanje 10000 \times

3.4 Particle size distribution

Plastic waste is a significant source of MPs in the environment. Larger plastic objects break down into smaller pieces and eventually become micro-particles. The fragmentation process heavily depends on structural integrity and mechanical properties of the polymer material, both of which may be altered by photo-oxidative degradation. Therefore, the pristine and the aged HDPE films were ground under the same conditions to observe the differences in the particle size distribution, and correlate them with the structural changes caused by their exposure to UV irradiation. Fig. 9 presents particle size distributions in terms of mass fractions (%) for HDPE/0, HDPE/14, HDPE/28, and HDPE/42. It can be seen that, in the case of HDPE/0, the obtained mass fraction of particles > 500 μm was 100%. On the other hand, in the cases of aged HDPE films, grinding under the same conditions yielded fractions with smaller sizes as well. Thus, photo-oxidative degradation caused

loss of mechanical properties and made HDPE films more prone to fragmentation into smaller particles. Consequently, mass fractions of largest particles (> 500 μm) follow the decreasing order HDPE/0 > HDPE/14 > HDPE/28. The HDPE/28 exhibited the highest brittleness due to its most pronounced fragmentation into particles of smaller size ranges and highest mass fraction of particles < 100 μm . It should be noted that a relatively modest increase in % mass fraction represents a major increase in terms of the number of particles in small size ranges. Although one might expect HDPE/42 to exhibit the highest brittleness based on FT-IR results, this was not the case according to the particle size distribution results presented in Fig. 9. It can be seen that HDPE/42 is characterised by a higher mass fraction of particles > 500 μm and lower mass fractions of all smaller particle ranges compared to HDPE/28. However, this could not be confirmed due to the small magnitude of the mass loss, which was in the range of the gravimetric error of the used scale. This change in particle size distribution indicated a change in the structure of the macromolecules of the HDPE polymer, such as chain scission, which allowed recrystallisation – “chemocrystallisation”. Since the formation of macromolecules with significantly lower mass increases crystallinity, this leads to higher brittleness as a result of an increased degree of photodegradation.²⁹

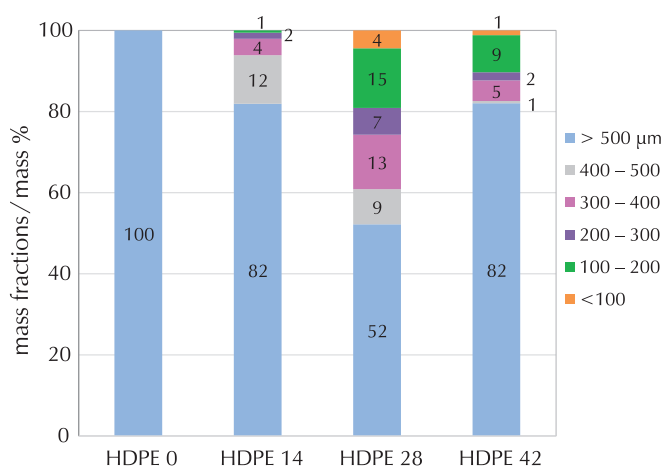


Fig. 9 – Particle size distributions (μm) and mass fractions (mass%) of HDPE ground films UV-irradiated 0, 14, 28, and 42 days

Slika 9 – Raspodjela veličina čestica (μm) te masenih udjela (mass%) za usitnjene HDPE filmove UV ozračenane tijekom 0, 14, 28 i 42 dana

4 Conclusion

This study has shown that environmental factors such as solar irradiation and temperature have strong effects on the surface of HDPE polymer. The results of FTIR analysis showed a significant change in surface chemistry, where new C=O and C–O bonds were formed because of degradation, while the calculated carbonyl index increased by three orders of magnitude. Degradation began slowly during the first 14 days of weathering, but progressed more rapidly thereafter. As a result, the hydrophilicity of

the surface increased, as shown by the contact angle measurements. Aged plastics were susceptible to increased fragmentation as was observed by grinding. This increased the risk of adsorption of inorganic and organic contaminants on the surface. Increased crystallinity (X_c) with prolonged UV ageing time indicated increased degradation of the studied samples. Increasing fragmentation of HDPE samples with ageing was also observed, indicating increasing crystallisation, confirmed by DSC, and brittleness, as confirmed by particle size distribution after cryogenic grinding. SEM images showed that, despite the obvious degradation after 42 days of ageing, the surface mostly exhibited a coherent structure with only occasional cracks. The tendency of degraded HDPE to fragment into MPs, combined with the increased possibility of adsorption of various pollutants, facilitates their transport into the environment.

ACKNOWLEDGEMENTS

We would like to acknowledge the financial support of the Croatian Science Foundation under the project Microplastics in water; fate and behaviour and removal, ReMiCRO (IP-2020-02-6033).

Popis kratica

List of abbreviations

HDPE	– high-density polyethylene – polietilen visoke gustoće
UV	– ultraviolet (irradiation) – ultraljubičasto (zračenje)
EU	– European Union – Europska unija
PET	– poly(ethylene terephthalate) – poli(etilen-tereftalat)
PVC	– poly(vinyl chloride) – poli(vinil-klorid)
LDPE	– low-density polyethylene – polietilen niske gustoće
PP	– polypropylene – polipropilen
PS	– polystyrene – polistiren
GHG	– greenhouse gas – staklenički plin
MPs	– microplastics – mikroplastika
FTIR	– Fourier-transform infrared spectroscopy – infracrvena spektroskopija s Fourierovom transformacijom
ATR	– attenuated total reflection – prigušena potpuna refleksija
C.I.	– carbonyl index – karbonilni indeks
SEM	– scanning electron microscopy – pretražna elektronska mikroskopija
DSC	– differential scanning calorimetry – diferencijalna pretražna kalorimetrija

References

Literatura

1. Global plastic market size value 2021–2030, May, 2022, URL: <https://www.statista.com/statistics/1060583/global-market-value-of-plastic/> (9. 12. 2022.).
2. Plastic Europe, Plastics – the Facts, 2021, URL: <https://plasticseurope.org/wp-content/uploads/2021/12/Plastics-the-Facts-2021-web-final.pdf> (15. 11. 2022.).
3. P. Eyerer Volker, G. Volker Gettwert, Properties of Plastics in Structural Components, in P. Eyerer (Ed.), *Polymers – Opportunities and Risks I. The Handbook of Environmental Chemistry*. Vol. 11. Springer, Berlin, Heidelberg, 2010, pp. 47–165, doi: https://doi.org/10.1007/978-3-540-88417-0_3.
4. R. Klein, Material Properties of Plastics, in R. Klein (Ed.), *Laser Welding of Plastics: Materials, Processes and Industrial Applications*. Vol. 12, Wiley-VCH Verlag, Weinheim, 2011, pp. 3–69, doi: <https://doi.org/10.1002/9783527636969.ch1>.
5. Ellen MacArthur Foundation, New Plastics Economy – Catalysing Action. 2017, URL: https://www3.weforum.org/docs/WEF_NEWPLASTICSECONOMY_2017.pdf (9. 12. 2022.).
6. The Pew Charitable Trusts and SYSTEMIQ, “Breaking the Plastic Wave: A Comprehensive Assessment of Pathways Towards Stopping Ocean Plastic Pollution”, 2020, URL: www.systemiq.earth/breakingtheplasticwave/ (1. 12. 2022.).
7. A. Shenoy, Rheometers for Polymer Melt Characterization, in A. Shenoy (Ed.), *Thermoplastic Melt Rheology and Processing*, Vol. 1, CRC Press, 1996, pp. 94–114, doi: <https://doi.org/10.1201/9781482295535>.
8. I. Kremer, T. Tomić, Z. Katančić, M. Erceg, S. Papuga, J. Parlov Vuković, D. R. Schneider, Catalytic pyrolysis and kinetic study of real-world waste plastics: multi-layered and mixed resin types of plastics, *Clean Technol. Environ. Policy* **24** (2022) 677–693, doi: <https://doi.org/10.1007/s10098-021-02196-8>.
9. V. Godoy, M. A. Martín-Lara, M. Calero, G. Blázquez, Physical-chemical characterization of microplastics present in some exfoliating products from Spain, *Mar. Pollut. Bull.* **139** (2019) 91–99, doi: <https://doi.org/10.1016/j.marpolbul.2018.12.026>.
10. Future of Reusable Consumption Models; World Economic Forum, July 2021, URL: https://www3.weforum.org/docs/WEF_IR_Future_of_Reusable_Consumption_2021.pdf (7. 10. 2022.).
11. A. Al Mamun, T. A. Eka Prasetya, I. R. Dewi, M. Ahmad, Microplastics in human food chains: Food becoming a threat to health safety, *Sci. Total Environ.* **858** (2023) 159834, doi: <https://doi.org/10.1016/j.scitotenv.2022.159834>.
12. D. Lithner, A. Larsson, G. Dave, Environmental and health hazard ranking and assessment of plastic polymers based on chemical composition, *Sci. Total Environ.* **409** (2011) 3309–3324, doi: <https://doi.org/10.1016/j.scitotenv.2011.04.038>.
13. M. Piccardo, F. Provenza, E. Grazioli, A. Cavallo, A. Terlizzi, M. Renzi, PET microplastics toxicity on marine key species is influenced by pH, particle size and food variations, *Sci. Total Environ.* **715** (2020) 136947, doi: <https://doi.org/10.1016/j.scitotenv.2020.136947>.
14. M. Renzi, A. Blašković, G. Bernardi, G. F. Russo, Plastic litter transfer from sediments towards marine trophic webs: a case study on holothurians, *Mar. Poll. Bull.* **135** (2018) 376–385, doi: <https://doi.org/10.1016/j.marpolbul.2018.07.038>.
15. T. J. Henman, Polymer degradation and stabilisation, in N. Grassie, G. Scott (Ed.), *Polymer Degradation and Stabilisation*; Cambridge University Press: Cambridge, 1988, pp. 1–222.

16. G. H. Hartley, J. E. Guillet, Photochemistry of Ketone Polymers. I. Studies of Ethylene-Carbon Monoxide Copolymers, *Macromolecules* **1** (1968) 165–170, doi: <https://doi.org/10.1021/ma60002a012>.
17. I. H. Craig, J. R. White, A. V. Shyichuk, I. Syrotynska, Photo-Induced Scission and Crosslinking in LDPE, LLDPE, and HDPE, *Polym. Eng. Sci.* **45** (2005) 579–587, doi: <https://doi.org/10.1002/pen.20313>.
18. M. Gardette, A. Perthue, J. L. Gardette, T. Janecska, E. Foldes, B. Pukánszky, S. Therias, Photo- and Thermal-Oxidation of Polyethylene: Comparison of Mechanisms and Influence of Unsaturation Content, *Polym. Degrad. Stab.* **98** (2013) 2383–2390, doi: <https://doi.org/10.1016/j.polymdegradstab.2013.07.017>.
19. B. Gewert, M. M. Plassmann, M. MacLeod, Pathways for Degradation of Plastic Polymers Floating in the Marine Environment, *Environ. Sci. Process. Impacts.* **17** (2015) 1513–1521, doi: <https://doi.org/10.1039/C5EM00207A>.
20. J. Almond, P. Sugumaar, M. N. Wenzel, G. Hill, C. Wallis, Determination of the carbonyl index of polyethylene and polypropylene using specified area under band methodology with ATR-FTIR spectroscopy, *e-Polymers.* **20** (2020) 369–381, doi: <https://doi.org/10.1515/epoly-2020-0041>.
21. J. Brandon, M. Goldstein, M. D. Ohman, Long-term aging and degradation of microplastic particles: Comparing in situ oceanic and experimental weathering patterns, *Mar. Pollut. Bull.* **110** (2016) 299–308, doi: <https://doi.org/10.1016/j.marpolbul.2016.06.048>.
22. B. Wunderlich, G. Czornyj, A study of equilibrium melting of polyethylene. *Macromolecules* **10** (1977) 906–913, doi: <https://doi.org/10.1021/ma60059a006>.
23. R. Panowicz, M. Konarzewski, T. Durejko, M. Szala, M. Lazinska, M. Czerwinska, P. Prasula, Properties of Polyethylene Terephthalate (PET) after Thermo-Oxidative Aging, *Materials* **14** (2021) 3833, doi: <https://doi.org/10.3390/ma14143833>.
24. R. G. W. Norrish, C. H. Bamford, Photo-Decomposition of Aldehydes and Ketones. *Nature* **140** (1937) 195–196, doi: <https://doi.org/10.1038/s41598-020-79701-4>.
25. Norrish Type I photoreaction (N04219). IUPAC Gold Book. IUPAC. URL: <http://goldbook.iupac.org/terms/view/N04219> (9. 12. 2022.).
26. J. M. Restrepo-Flórez, A. Bassi, M. R. Thompson, Microbial Degradation and Deterioration of Polyethylene – A Review, *Int. Biodeterior. Biodegrad.* **88** (2014) 83–90, doi: <https://doi.org/10.1016/j.ibiod.2013.12.014>.
27. A. Chamas, H. Moon, J. Zheng, Y. Qiu, T. Tabassum, J. H. Jang, M. Abu-Omar, S. L. Scott, S. Suh, Degradation Rates of Plastics in the Environment, *ACS Sustain. Chem. Eng.* **8** (2020) 3494–3511, doi: <https://doi.org/10.1021/acssuschemeng.9b06635>.
28. X. Chen, G. Hou, Y. Chen, K. Yang, Y. Dong, H. Zhou, Effect of molecular weight on crystallization, melting behavior and morphology of poly(trimethylene terephthalate), *Polym. Test.* **26** (2007) 144–153, doi: <https://doi.org/10.1016/j.polymer-testing.2006.08.011>.
29. W. F. Smith, Principles of Materials Science and Engineering, Vol. 3., McGraw-Hill College, New York, USA, 1995, pp. 890–896.

SAŽETAK

Od makro do mikroplastike; utjecaj fotooksidativne degradacije

Josipa Papac Zjačić,^a Magdalena Vujasinović,^a Marija Kovačić,^a Ana Lončarić Božić,^a Hrvoje Kušić,^{a,b} Zvonimir Katančić^a i Zlata Hrnjak Murgić^a

Utjecaj plastičnog otpada na okoliš, ljudsko zdravlje te ekosustav jedno je od najvažnijih pitanja današnjice. Nakon što se ispusti u okoliš, otpad je izložen različitim okolišnim utjecajima koji mogu dovesti do narušavanja cjelovitosti strukture, a posljedično i do fragmentacije na manje dijelove. U ovom su radu istraživani učinci simuliranog UV starenja na površinska svojstva i fragmentaciju filmova polietilena visoke gustoće (HDPE). HDPE filmovi pripremljeni su od polimernih granula te potom starni 14, 28 i 42 dana pod utjecajem simuliranog UV zračenja. Uzorci su karakterizirani prije te nakon svakog razdoblja ozračivanja da bi se utvrdile strukturne i površinske promjene. Na temelju FTIR spektara ustanovljena je pojava karbonilnih (C=O) i ugljiko-kisikovih (C–O, O–C=O, C–O–O–) skupina kao rezultat fotodegradacije HDPE-a. Promjena polarosti površine s vremenom UV ozračivanja određena je mjerenjem kontaktnog kuta, dok je morfologija površine analizirana SEM mikroskopom. Rezultati su ukazali na znatno povećanje karbonilnog indeksa te hidrofilnosti, kao i povećanu lomljivost kao rezultat visokog stupnja fotodegradacije nakon 28 i 42 dana UV zračenja. Različita raspodjela veličine čestica dobivena mljevenjem materijala upućuje na to da su starni HDPE filmovi skloniji fragmentaciji u čestice mikroveličina.

Ključne riječi

Plastični otpad, HDPE filmovi, fotodegradacija, hidrofilnost-hidrofobnost, fragmentacija

^a Zavod za polimerno inženjerstvo i organsku kemijsku tehnologiju, Sveučilište u Zagrebi, Fakultet kemijskog inženjerstva i tehnologije, Trg Marka Marulića 19, 10 000 Zagreb

^b Sveučilište Sjever, Trg dr. Žarka Dolinara 1, 48 000 Koprivnica

Izvorni znanstveni rad
Prispjelo 23. siječnja 2023.
Prihvaćeno 2. svibnja 2023.